A review of 30 years of french instrumented dynamic cone penetrometer panda

Miguel Angel Benz Navarrete[1#], *Pierre* Breul[2] *Gabriel* Villavicencio[3], *Philippe* Moustan[4]*and Luc* Teissier[4]

[1]*Sol Solution, Research, Innovation and Development department, Riom, France*
[2]*Institut Pascal, Université Clermont Auvergne, Aubière, France*
[3]*Pontificia Universidad Católica de Valparaíso, Chile*
[4]*Sol Solution, Riom, France*
[#]*Corresponding author: mbenz@sol-solution.com*

ABSTRACT

Dynamic penetrometer is a worldwide practice in geotechnical exploration and the French Panda (1) lightweight variable energy is the most developed device nowadays. Widely used in France and other countries, The Panda penetrometer is relatively unknown for characterizing surface soils domain and the possibilities it offers. In this article, the authors offer a brief review of the principle of measurement, its uses, advantages and disadvantages calibration, and interpretation, as well as the different relationships with other in-situ test (CPT, SPT…) and some geotechnical parameters. A summary of the works that can be found and that are based on this technology is also presented. The overall aim is to provide the reader with a basic historical document for a better understanding of the operation and analysis of the results obtained with this device, enabling it to be integrated, as a complement, into in situ investigation campaigns.

Keywords: Dynamic Penetrometer, Panda, instrumented DCP, soil characterization, in-situ test, compaction control, field correlation.

1. Introduction

Dynamic penetration tests (DPT) are a worldwide technique for soil characterization. Due to its rapid implementation, affordability, and suitability for a large range of soils, DPT are present in many countries (Sanglerat, 1972). This is certainly the oldest one technique for geotechnical soil characterization. According to literature review presented by (Massarch, 2014), the first known experiences of the DPT date back to the 17th century in Europe. N. Goldmann described a dynamic penetrometer as a method of hammering a rod with a conical tip where penetration per blow can be recorded to find differences in the soil stratigraphy (Goldmann, 1699). At the beginning of the 20th century, the first major development also took place in Germany with the development of a lightweight dynamic penetrometer, the Künzel Prüfstab, later standardized in 1964 as the "Light Penetrometer Method".

With the European development of DPTs and due to its simplicity, numerous developments have occurred. Scala developed in Australia the Scala dynamic penetrometer (Scala, 1956), which has been widely used for design of pavement. Sowers and Hedges developed the Sowers penetrometer, for in-situ exploration and to assess the bearing capacity of shallow footings (Sowers & Hedges, 1966). Webster et al. and the US Army Corps of Engineers developed the dual mass DCP (Webster et al., 1992), well known in North America and many other countries (ASTM-D6951-18, 2015; Salgado & Yoon, 2003). The Mackintosh probe was developed recently by Sabtan and Shehata (Sabtan & Shehata, 1994). The lightweight penetrometer was standardized in Germany in 1964.

Moreover, the low driving energy and limited probing depth led to the development of heavier devices in Europe and the USA (SPT, Borros, Andina…) (Broms & Flodin, 1988). Several generations of DPTs have succeeded one another, and today, a wide variety of them can be found (Sanglerat, 1972). Despite the wide variety of DPTs developed over the last century, the fundamental principle, equipment, and technology remain unchanged from those described by (Goldmann, 1699) and the Künzel Prüfstab (Künzel, 1936). Indeed, unlike the CPT (Lunne et al., 1997; Massarch, 2014), which has undergone significant technological development, DPTs have not embraced these advances and continue to rely on old and rudimentary techniques.

It was only at the end of the 1980s that the first major improvements in design, measurement principles, and equipment took place. "In France, engineer and researcher Roland Gourvès developed the first instrumented lightweight dynamic variable energy penetrometer: the Panda (from French Pénétromètre Autonome Numérique Dynamique Assisté par ordinateur) (Benz-Navarrete, 2009; Benz-Navarrete et al., 2020a; Gourvès, 1991; Gourvès & Zhou, 1997; Langton, 1999). However, despite being widely used in France, Europe, America, and many other countries around the world, the Panda technology remains unknown to many practitioners and contractors.

(a) (b) (c)

Figure 1. Instrumented lightweight dynamic penetrometer Panda (Gourvès, 1991). (a) first génération of the devices mesureing kinect energy just before the blow, (b) second generation (current comercial version) mesuring strain energy just after the blow, (c) Main components of the Panda.

2. The PANDA penetrometer

Created in 1989, the test belongs to the family of lightweight dynamic penetrometers, whose principle consists of driving a cone fixed to the lower end of a rod into the soil. The main idea was to design an instrumented and autonomous device at low cost, lightweight, and small, yet with sufficient penetration power to test most soils to a depth of a few meters. The implementation of variable energy, which allows the driving energy to be adapted according to the hardness of the soil, is one of the fundamental principles and the main originality of the device. Energy variation is achieved by using a standard manual hammer and adjusting the intensity of the blow.

For each blow, the energy is directly measured by sensors located in the anvil, while other sensors simultaneously measure the cone penetration. These measurements are stored and analyzed in real-time by a specially designed Human-Machine Interface (HMI). The cone resistance *qd* s calculated automatically using the Dutch formula (Butcher et al., 1996; ISO-22476-2, 2005a; Powell, 2017; Sanglerat, 1972).

2.1. Historical background

The instrumented variable energy lightweight dynamic penetrometer was designed in 1989 (Gourvès, 1991). The work began in the 1980s under the direction of Roland Gourvès at C/U/S/T (Centre Universitaire des Sciences et Techniques) in Clermont Ferrand. Subsequently, a dozen studies were conducted between 1983 and 1991 to establish the fundamental principles of the device and to evaluate its technical and practical feasibility, including studies on repeatability. Other research was carried out to define operating modes, applications, and establish correlations with other geotechnical tests. (Turchet, 1983; Barrere, 1984; Imbault, 1985; Labbé, 1988; Goblet, 1989; Poix, 1990; Bustillo, 1990; Mathieu, 1990; Barjot, 1991... cited by (M. A. Benz Navarrete et al., 2013)). In 1991, the first version of the device was launched. Since then, three versions of the device have been developed (Benz-Navarrete, 2009; Escobar Valencia, 2015; Gourvès, 1991; Gourvès & Zhou, 1997; Zhou, 1997).

a) First generation: Panda 1. The first generation was created in the early 90s. In this concept, the impact energy (kinetic energy) is measured precisely at the moment of impact using Hall-effect sensors installed in a mobile steel anvil. Additionally, the settlement of the cone after each blow is measured with a digital encoder The cone resistance is immediately computed using the Dutch formula (Gourvès, 1991; Gourvès & Zhou, 1997; Langton, 1999; Zhou, 1997). The hammer weighs 2.5 kg and is made entirely of steel.

b) Second generation: Panda 2. In this version, developed from 2002 onwards, the first major innovation in dynamic penetrometer was introduced: the strain wave energy is measured by means of strain gauges just after each blow (Benz-Navarrete, 2009). The energy is computed using the simplified EF2 method (Schmertmann & Palacios, 1979). The hammer has been lightened and modified to produce a semi-sinusoidal compressional wave at each blow. Cone resistance is computed using the Dutch Formula, and a shock pendulum was employed to establish the relationship between the kinetic energy and the strain wave energy.

c) Third generation: Panda 3. The studies carried out on the second version led to a fundamental analysis: How can the advances made over the last 20 years in pile driving and dynamic testing of materials using the Hopkins bar be integrated into the dynamic penetrometer? The third and more sophisticated version of the device was born and developed since 2010. Here, three types of sensors are installed (accelerometers, strain gauges and displacement) and the wave equation is

automatically solved to separate the fundamental waves propagating in the penetrometer just after each blow. In addition to the cone resistance, still calculated using the Dutch formula, for each blow, the dynamic cone load curve (DCLT) is plotted using wave reconstruction methods. As presented by (M. Benz Navarrete et al., 2021; Benz-Navarrete, 2009), from DCLT curve, soil strength, dynamic stiffness, shear modulus, shear wave velocity… are computed.

In all three versions, the measurement and processing routines are fully automated, the drive energy still "variable", and the main result, cone resistance, is always computed using the Dutch Formula, as recommended by (ISO-22476-2, 2005a).

2.2. Measuring principle

The principle is simple: it involves manually driving rods into the ground by varying the intensity of the hammer. At each blow, drive energy and cone penetration are measured. The dynamic cone resistance *qd* can be obtained using the Dutch Formula, derived from a general driving formula based on a simple conservation of energy principle. In fact, theoretically it can easily be demonstrated that to drive a penetrometer of mass *P* (over a distance *e* into a perfect elasto-plastic soil having a tip/base resistance *Qd*) by means of a mass *M* which falls from a height *H* and strikes the penetrometer at a speed $v_0=(2gH)^{1/2}$, both being rigid, we can establish the following relationship:

$$Q_d e = k_1 MgH - k_2 \frac{Q_d e'_p}{2} - k_3 MgH \frac{P}{(M+P)} + (M+P)ge \quad (1)$$

with k_1MgH (or $k_1(1/2Mv_o^2)$) the input drive energy, where k_1 represents the efficiency of the penetrometer driver thus $k_1 \leq 1$. The term $k_2(1/2Qd\, e'_p)$ represents the energy losses due to the elastic shortening e'_p of the penetrometer, as well as those taking place at the hammer/anvil and anvil/rod interfaces, thus coefficient $k_2 \geq 1$. Expression $k_3MgH\ P/(M+P)$ represents the losses energy due to the inelastic impact of the hammer *M*, where k_3 is a function of Newton's coefficient of restitution ε, $k_3 = (1-\varepsilon^2)$, and k_3 is equal to 1 for a perfectly inelastic shock and 0 for a perfectly elastic shock. Finally, $(M+P)ge$ the work of inertial force of the assembly just after the impact.

Dutch formula (eq. 2) is obtained by considering that: a perfectly inelastic shock ($k_3=1$); no energy loss during each blow ($k_1=1$) and neglecting both energy losses due to elastic shortening and inertial work after blow.

$$q_d = \frac{Mgh}{Ae}\frac{M}{(M+P)} \quad (2)$$

where $qd = Qd/A$ and *A* is the cross section of the tip of the cone. Other driving formulas have been derived and proposed from the general driving expression (eq. 1). Other formulas can be obtained from the general pile-driving formula. However, it has been shown that the Dutch formula provides a simple and reliable estimator of soil resistance *qd* and its use is recommended for the interpretation of DPT test. Early on, (Waschkowski, 1983), recommended the use of the Dutch formula to obtain comparable results with those obtained with CPTs. Recently, (Powell, 2017), based on (Butcher et al., 1996), show that the use of drive formulas, such as Dutch formula, improves the quality of DPT analysis (ISO 22476-2) and makes them comparable with those obtained through CPT.

In the case of the Panda, it has been decided to use the Dutch formula to normalize the measurements taken at variable engine power. Additionally, it is simple to implement, reproducible, and recommended by ISO standards. (ISO-22476-2, 2005b).

Table 1. Main features of dynamic penetrometers

	SPT	Chinese DPT	CPT	Panda
Drive mode	dynamic	dynamic	sinking	dynamic
M (kg)	63,5	120	-	1,76
H (m)	0,76	1	-	variable
V_i (m/s)	3,9	4,4	0.02	2 to 12
D_r (mm)	50	60	35	14
D_t (mm)	50,5	74	35.3	22,5
D_t/D_r	1,0	1,2	~1,0	1,6
A_t (cm^2)	20	43	10	4
Cone angle	90°	60°	60°	90°
E_{theo} (J)	473	1177	-	3-126
Pp (kJ/m^2)	236	274		7,5-315
Penetration rate	variable	variable	20mm/s	variable
Max. depth (m)	< 200	< 30	20 - 30	7
Instrumentation	optional	optional		included
Energy meas.	(option)	(option)	included	included
Meas. type	-	-	Strain	Strain
In-situ meas.	N_{SPT}	N_{30}	Force	Drive energy
Cone resistance			Force/A_t	Dutch formula
Accessibility	+	+	+	+++
Investment	€€€	€€	€€€€	€
GPS	Non	Non	Yes	Included
Software assoc.	Non	Non	option	included
Weight (kg)	> 1000	> 1000	> 1000	~23,5

2.3. Equipment

Panda is composed by six elements: hammer, instrumented anvil, rods, conical tips, central acquisition unit (UCA) and HMI (TDD) (Fig. 1.c). The sections of the cones used are respectively 2cm² or 4cm². The former are mainly utilized for compaction control in tests with depths less than 1.50m, while the latter are employed for geotechnical investigations involving greater depths. As these cones overflow, they help minimize the skin friction along the rods.

The UCA is an electronic device designed to drive, centralize recordings, and process them before transmitting to the TDD. This is an electronic HMI device that facilitates communication between the operator and the device. It enables the operator to define sites and tests, save measurements, visualize surveys, and configure various parameters.

The total weight is less than 20kg, which makes it easily transportable and easy to handle.

2.4. Data processing and analysis

One of the great advantages of the Panda is its ability to conduct precise layer-by-layer exploration, ranging from very low to high resistance, achieved by controlling

the hammering energy and adapting the intensity of hammering. The measurements obtained enable the establishment of penetrograms with extremely high spatial resolution, as illustrated in Fig. 2.

2.4.1. Signal processing.

Signal processing is necessary on the raw penetrometer data to filter the signal and enhance its quality. It is common to perform clipping (*removal of outliers*) then smoothing and regularization. For penetrogram clipping, this is analyzed by windows of fixed length L_W, which are not overlapped. Inside each window, values greater than x times the variance will be eliminated or replaced by the mean value.

Concerning penetrogram smoothing, two techniques are recommended: averaging by sliding window of fixed length W_j (i.e.: W_j = 50mm) or the Kalman filter. In order to reduce the number of values, it is possible to regularize the signal by consecutive, non-overlapped windows of constant length W_j (i.e.: W_j = 100mm), such that:

$$qd^* = \frac{\sum qd_i \cdot e_i}{\sum e_i} \quad (3)$$

with qd_i the resistance measurements in the window Wj and e_i *the* measured penetrations. Fig.2.a shows an example of raw, clipped, smoothed, and regularized penetrograms recently obtained in a leaching pile (Chile).

2.4.2. Skin friction correction

In a cone dynamic penetrometer, skin friction, along with factors such as the drive energy transmitted to the rods and the position of the groundwater table, can significantly influence results. To mitigate this effect in the field, methods such as bentonite drill mud injection or the use of overflowing tips are often employed. In the latter case, which is the most common, the ratio between cone and rod diameter must be at least 1.35. In the case of the Panda test, which utilizes 22.5 mm diameter cones and 14 mm rods, this ratio is 1.6.

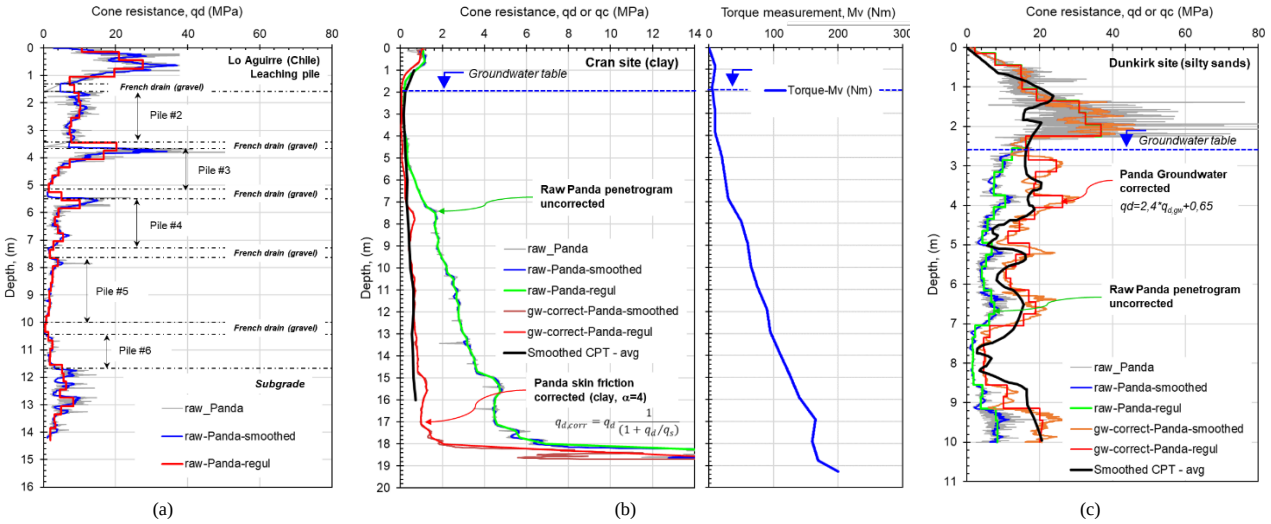

(a) (b) (c)

Figure 2. Panda measurement penetrograms. (a) Example of signal processing *(raw, smoothed and regularized signal)*; (b) Correction of skin friction from torque measurements and (c) Effects of the groundwater table and example of correction.

However, it is recommended to measure the torque (Mv) with a dynamometer key. In fact, it has been shown that cone resistance qd increases when the torque (Mv) increases (penetration e per blow decreases, when the torque measurement increases). To take this into account, the measured values of qd can be corrected $qd_{,corr}$ from torque measurements values (Mv) according to:

$$E_s = \frac{2\alpha M_v \Delta e}{D_R}; then \rightarrow q_s = \frac{E_s}{A_t \Delta e} \quad (4)$$

$$q_{d,corr} = q_d \frac{1}{(1 + q_d/q_s)} \quad (5)$$

where Es is the energy required to mobilise a penetration Δe, D_R is the rod diameter q_s the equivalent cone resistance associated to the skin friction, qd the measured cone resistance and $qd_{,corr}$, the corrected cone resistance. The coefficient α depends on the type of soil (α = 1 for sand, 2 for silts and 4 for clays). In the Fig. 2.b an example of corrected measurements performed with Panda are presented. CPT measured profiles are also shown.

2.4.3. Boreholes below the water table

Given the dynamic nature of the DCP test, in some cohesionless soils, the presence of the water table can have significant effects on the measured qd. For fully drained sand, qd can increase significantly, by up to 250%, compared to fully submerged sand. To take account of the effects of water content, we recommend using the following expression, based on the recommendations of ISO 22476-2:

$$q_d = a_1 q_{d,gw} + a_2 \quad (6)$$

where $qd_{,gw}$ is the cone resistance measured below de water-table and a_1, a_2 are dimensionless coefficients. Empirical studies have shown that $a_1 \in [1{,}95 - 2{,}85]$ and $a_2 \in [0{,}65 - 1{,}05]$. In practice, for clean, uniform sand, it is assumed that $qd \approx 2{,}5 qd_{,gw}$. Fig. 2.c shows an example of penetrograms obtained in a sandy site, with qd values above and below water table. Cone resistance measured with CPT is also presented. The values a_1=2.4 and a_2 = 0.65 are used to correct the $qd_{,gw}$ values.

2.4.4. Effects of overburden pressure

Since the measured value corresponds to the net resistance *qd*, it is recommended, for some analyses, to consider the overburden pressure as follow.

$$qd_1 = qd\left(\frac{p_a}{\sigma'_{vo}}\right)^m \quad (7)$$

with *qd* cone resistance (Mpa), p_a atmospheric pressure (1 atm ≈ 103 Kpa ≈ 0.1 Mpa), σ'_{vo} the effective stress of the soil mass and *m* the stress normalization exponent (for sandy soils asumed equal to 0.5).

(Villavicencio et al., 2018, 2021) studied the effects of overburden pressure on *qd* for mine waste soils (, confirming the above relationship (eq. 6) and the exponent m=0.5. As part of its studies to develop a method for assessing slope stability (Athapaththu et al., 2007, 2015, 2016; Tsuchida et al., 2011) show the effects of vertical confining pressure on results for Masado's residual dsandy soils. More recently, in a more exhaustive calibration chamber study, (López Retamales, 2022; Retamales et al., 2021) confirmed the good agreement of expression above. The study here focused on the Fontainebleu and Hostun sands.

3. Field applications

Panda technology is mainly used for soil investigation at shallow depths; for compaction control of road embankments, dikes, earth dams, etc.; for assessment of the bearing capacity of wasteland or road earthworks; for assessment of the risk of liquefaction of earth dams or tailings dams.

3.1. Shallow soil characterisation

Investigations with the Panda can reach depths of 6 to 7 meters, or even more in some cases, depending on the soil resistance and the absence of skin friction along the rods. This depth capability is sufficient to address a significant number of shallow geotechnical problems, typically in the range of 0-100 kPa.

3.1.1. Layer detection

One of the significant advantages of the device is its ability to continuously record soil resistance. The resulting penetrogram offers valuable insights into the stratigraphy of shallow formations. Based on this data, various methods have been applied to detect ground stratigraphy from the test results. The most common method is the 'empirical' approach, where the operator defines the boundaries between each stratum based on variations in cone resistance observed in the penetrogram. (Chaigneau, 2001) proposes an automatic stratigraphy identification technique: the cone resistance *qd* follows a log normal law and the coefficient of variation is constant for a homogeneous material. More recently, in a more exhaustive work, (Sastre Jurado, 2018; Sastre Jurado et al., 2016, 2021) proposes the application of the T-ratio, Intra-class coefficient and Bartlett test techniques, which are based on the analysis of penetrograms by sliding window. A very good agreement between empirical analysis and automatic predictions from Panda penetrograms was obtained.

3.1.2. Spatial modelling of soil variability

Another area of application for the device is the assessment of the spatial variability of soils. With almost continuous recording at depth, and given the simplicity of conducting the tests, it is easy to apply geostatistical analysis and modelling methods to assess the site's hazard. Very early, (Deplagne & Bacconnet, 1993) used Panda to carry out a structural analysis of a clay dike using a geostatistical approach. Later, (Chaigneau, 2001) applied these same concepts to the spatial modelling of trench compaction properties. In addition, (Lepetit, 2004; Villavicencio, 2009; Villavicencio et al., 2011, 2022) proposes, based on (Deplagne & Bacconnet, 1993) work, to apply these methods to the spatial modelling of the liquefaction safety factor and compaction control of earth dam and tailings dams. For its part, (Athapaththu et al., 2016; Tsuchida et al., 2011) use Panda data to model soil behaviour and cone resistance features as part of the diagnosis of the Masado's slope. More recently, (Sastre Jurado, 2018; Sastre Jurado et al., 2016, 2021) proposes a probabilistic approach to modelling and predicting shallow soil properties based on geostatistical and machine learning techniques.

3.1.3. Empirical correlations

Numerous investigations have been conducted to establish empirical correlations between the cone resistance *qd* and various physical, state, or mechanical properties of the soil, as well as the results obtained from other in-situ tests.

For sand and cohesionless soils, dynamic penetrometers are widely used to assess its state parameters (D.R., dry density, void index…) and mechanical parameters (angle of friction). Concerning relative density (D.R.), (Villavicencio et al., 2016, 2021, 2022) proposes, for silty sands, an empirical model was adapted by using a simple regression on all the pairs of experimental data (qd_1, *DR*).

$$DR = 28{,}5\ln(qd_1) - 65{,}4\ ;\ 20 \le qd_1 \le 326 \quad (8)$$

where qd_1 is cone resistance *qd* coorected from overburden pressure effects. More recently, (López Retamales, 2022; López Retamales et al., 2021) based on tests carried out in a calibration chamber using dry, saturated Fontainebleau and Hostun sands, proposes the following relationship between *DR* and normalized qd_1.

$$DR = a_1\ln(qd_1) + a_2 \quad (9)$$

For dry condition, the a_1 value is 33.5 or 23.4, while the a_2 value is 23.7 or 26 for fontainebleu and hostun sand respectively. For saturate state, the a_1 value is 29.4 or 31.2, while the a_2 value is 15.9 or 13 for fontainebleu and hostun sand respectively.

(Athapaththu et al., 2015; Tsuchida et al., 2011) proposes a relationship between void index (e), degree of saturation (*Sr* in %) and cone resistance qd_5 (qd_5 is defined as cone resistance for 5 kPa overburden stress and can be as follow $qd_5 = qd - 0.01*(\gamma_t*z - 5)$).

$$e = 1.19 - 0.084\ln(qd_1) - 0.007S_r \quad (10)$$

In addition, the Panda developers propose the following relationship between cone resistance *qd*, dry γ_d

and bulk γ_T densities, for sands and all soils, above the water table, respectively:

$$\gamma_d = 0.18 \log\left(\frac{q_d}{p_a}\right) + 1.39 \text{ (sands)}$$
$$\gamma_d = 0.25 \log\left(\frac{q_d}{p_a}\right) + 1.33 \text{ (all soil)} \quad (11)$$
$$\frac{\gamma_T}{\gamma_W} = 0.36 \log\left(\frac{q_d}{p_a}\right) + 1.43 \text{ (all soil)}$$

Concerning the evaluation of the friction angle ϕ', (Villavicencio et al., 2011) proposes the expression:

$$\emptyset' = 14.79 + 5.54 \ln(qd_1) ; 10 \leq qd_1 \leq 280 \quad (12)$$

(Athapaththu et al., 2015; Tsuchida et al., 2011) proposes a relationship between friction angle ϕ', apparent cohesion (c_d in kPa), cone resistance *qd* and degreee of saturation (*Sr*) of the Masado soils given by :

$$\emptyset' = 29.9 + 1.61 \ln(qd_5) + 0.142S_r \quad (13)$$
$$c_d = 10.6 + 1.19 \ln(qd_5) + 0.041S_r \quad (14)$$

For fine cohesive soils, such as clays and silts, the most important parameter in the field is undrained shear strength, notes s_u. Dynamic penetration tests have long been used to estimate the value of s_u. There is a very good relationship between *qd* and s_u.

$$s_u = \frac{q_d - \sigma_{vo}}{N_{kt}} \quad (15)$$

With σ_{vo} the vertical pressure and N_{kt} the correlation factor as a function of soil plasticity. Generally, it can be assumed $s_u = qd$ /(15 to 20) (Langton, 1999; Zhou, 1997).

Table 2. Estimation of the undrained shear strength s_u

Coeff.	Plasticity index (IP)			
	10 to 12	12 to 25	25 to 40	> 40
N_{kt}(*)	11	13	17	23

(*) *with* $N_{kt} \approx 0.285*IP + 7.64$

Panda & SPT relationship.

Despite the high variability in results obtained with the SPT probe due to factors such as apparatus type, drilling effects, energy corrections, and rod length, there exists a strong correlation between the cone resistance *qd* and the number of blows N_{SPT} from the SPT test.

Table 3. Summary of the N_{SPT}-*qd* correlation coefficient

Soil	α
Organic clays	1,8 to 2,4
Clays	2,2 to 3,0
Silt, clayey silts and silt mixtures	2,8 to 3,6
Silty sand, clay sand, clay sand	3,0 to 4,5
Sand, sandy gravels	4,4 to 6,8

The correlation coefficient α primarily depends on the soil type.

$$\frac{(q_d/p_a)}{N_{SPT}*} = \alpha \quad (16)$$

with *qd* the cone resistance (Mpa), p_a the atmospheric pressure (0.103 MPa), N_{SPT}^* the SPT value (*assumed near to N_{60}) and α the *SPT-qd* correlation coefficient. (Langton, 1999) proposes a coefficient α of between 1,0 and 1,95, based on comparative tests conducted on predominantly clay soils. Recently, (Angelim et al., 2016) proposes a correlation coefficient α equal to 2.73 for clayey soils. For silty sand, (Sanhueza & Villavicencio, 2010; Villavicencio, 2009)has obtained a correlation coefficient of 2,25.

Panda & CPT relationship. Various studies have demonstrated a strong correlation with CPT (cf. Fig. 2). (Benz-Navarrete et al., 2020b) presents a summary of the work reported in the literature and proposes :

$$q_c = 1.06\, q_d - 0.21$$
$$0.87 < \frac{q_c}{q_d} < 1.11 \quad (17)$$

This correlation is valid for most soils ($D_{max} < 50mm$), for *qd* values greater than 0.4Mpa and less than 50Mpa, and above the water table.

Panda & dual mass DCP relationship. "Since the work of Scala (1956), the dynamic penetrometer DCP has been widely utilized for the design and control of shallow foundations and pavement structures. The US Army Corps of Engineers has developed the dual mass DCP, known as ASTM 6951, which is extensively used in America and worldwide. This DCP features a dual mass hammer (4.6kg and 8kg) and a conical tip with an area of 3.14cm² and an apex angle of 60°. Due to their great similarity, a strong correlation has been demonstrated between the cone resistance *qd* and the penetration index IDCP. (Langton, 1999; Lopez Retamales et al., 2019).

$$q_d = \alpha IDCP^{-1} + \beta \quad (18)$$

with *qd* the cone resistance Panda (Mpa), *IDCP* the penetration index in (mm/blow), α and β the correlation coefficients (Table 5).

Table 4. Panda-dual mass DCP relationship (*qd-IDCP*)

Type of mass	α	β
DCP weight of 4.6Kg (R^2 0·87)	62.4	0.34
DCP weight of 8.0Kg (R^2 0.83)	108.7	0.27
General relationship (average)	97.8	0.31

Panda & DPL, DPH and DPSH relationship. In Europe, the use of dynamic penetrometers is described in Eurocode 7 and their main characteristics presented in (ISO-22476-2, 2005b). DPL, Borros (DPH) and DPSH-B are widely used. Given their geometric characteristics and the test procedure, there is a good correlation between the values of cone resistance *qd* and the results of the DPL (N_{10}), DPH (N_{10}) and DPSH-B (N_{20}) tests.

$$q_d = N_{xy}(a * L_r + b)^{-1} \quad (19)$$

Table 5. Panda-ISO 22476 penetrometer correlation (*qd-*N_{xy})

Type of penetrometer	*Coefficients*	
	a	*b*
DPL, $N_{xy} = N_{10}$	0.62	4.05
DPH, $N_{xy} = N_{10}$	0.07	0.88
DPSH-B, $N_{xy} = N_{10}$	0.08	1.18

In terms of cone resistance *qd*, it can be assumed that:

$$q_d = [0.88 - 0.98] q_{d,DPT} \quad (20)$$

where *qd* is cone resistance measured with Panda, $qd_{,DPT}$ is the cone resistance, obtained through Dutch formula using DPT ISO 22476-2 penetrometers.

Shear wave velocity Vs correlation. The development of shear wave velocity measurements for shallow soils has led to the implementation of many comparative tests, mainly including MASW. The Panda manufacturers, without citing the external source, propose the following relations as a first approach.

$$\begin{aligned} &\textit{All soils} && Vs = 113.5{q_d}^{0,34} \\ &\textit{Clays and silt} && Vs = 141.5{q_d}^{0,29} \\ &\textit{Sand} && Vs = 125.5{q_d}^{0,28} \\ &\textit{Gravels} && Vs = 110{q_d}^{0,29} \end{aligned} \qquad (21)$$

whit *Vs* the shear wave velocity in m/s and *qd* cone resistance in MPa. Recently, (Kang et al., 2023) proposes a *Vs*-*qd* relationship for railway ballast and fouled ballast as $Vs=25.47*qd^{0.79}$. However, a more suitable ratio for this type of soil is $Vs=87.5*qd^{0.31}$.

3.2. Compaction control

One of the most important uses of the device in France is quality assurance/quality control (QA/QC) of earthworks compaction. Although traditionally, compaction control is conducted by measuring the dry density and comparing it to the optimum Proctor value, control using the dynamic penetrometer has developed over the past thirty years. It involves comparing the penetrogram obtained with a pair of reference curves, q_R, and q_L, corresponding to the cone resistance *qd* that should be obtained if the compaction was satisfactory.

The q_R, and q_L curves are obtained from calibration curves, determined in the laboratory, but also in situ (NF P 94-105). The calibration is based on establishing the relationship between cone resistance *qd* and dry density γ_d. In fact, (Chaigneau, 2001; Espinace et al., 2007; Jayawickrama et al., 2000; Livneh & Livneh, 2013; Villavicencio et al., 2022; Zhou, 1997) have shown that for a given soil and variable water content *W*, there is a one-to-one relationship between *qd* and γ_d.

$$\gamma_d = A(w) + Bln(qd) + C \qquad (22)$$

with *A*, *B* and *C* the calibration coefficients for a given soil. At present, these values have been established for about forty soils, thus constituting an important database. Fig. 3 shows the *qd*-γ*d*-*w* database for thirty-eight different soils. Each point represents a soil sample at different density and water content. Here, the cone resistance represents the average value measured for all soil samples.

Compaction control with Panda is actually standardized in France, Morocco, and Chile (AFNOR, 2012; IMANOR, 2019; INN-NCH3261, 2012) for:

- Control of layer thickness and depth of compaction,
- Control of compaction layer by layer or as a whole
- Control of bearing capacity (CBR) of subgrades
- Optimization of compaction processes (test bed, number of passes, layer thickness, etc.)
- Determination of unusual areas in earthworks,
- Survey of slopes areas

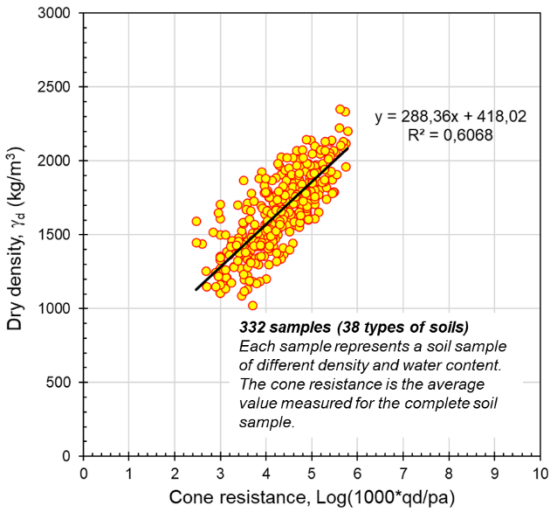

Figure 3. Panda compaction database. Dry density and cone resistance measurements for differents soils comapcted at different density and at different water content.

Finally, based on relationship proposed by (ASTM-D6951-18, 2015) and the relationship between cone resistance and DCP dual mass, various studies have established a correlation between cone resistance *qd* and CBR value determined according to the recommendations of ASTM 6951.

$$CBR = \alpha \cdot (qd)^{\beta} \qquad (23)$$

Where α and β are the correlation coefficient and depend on the type of soil.

Table 6. Estimate of the CBR bearing capacity index from qd

Type of soil	α	β
All soil	1,56	1,10
Very plastic clays and silts	3,27	1,00
Clays and silts of low plasticity (CBR< 10)	0,304	2,00

4. Conclusions

After 30 years since its creation, the French penetrometer Panda is now present inmore than 100 countries around the world. Panda is currently used by design offices, public organizations, private companies, research centers, universities... Nearly 4000 copies have been distributed, making it one of the most widely used devices for in-situ test and QA/QC of earthworks.

Its main applications are the characterisation of surface soils, the diagnosis and control of earthworks and the control of backfill compaction.

This prospecting method is very practical, fast and efficient for the auscultation of soil surface formations. In addition to its simplicity and speed of use, the repetitiveness, reliability and low variability of the results make this penetrometer a suitable tool for prospecting and mapping campaigns that seek to determine the spatial variability of soil mechanical behaviour in the field, even in areas of difficult access. This is a very interesting tool, ideal for easily completing the characterisation of surface

soils in addition to conventional tests, which are more expensive and more complex.

The Panda represents a very important advance in technology. Studies carried out over the last 30 years have made it possible to define calculation methodologies based on the use of the cone resistance *qd* of the device and to assess orders of magnitude of the intrinsic parameters of the soils under investigation.

Although the device has already been standardised in France for compaction control, the process of proposing a standard enabling this technique to be included in soil investigation and the preliminary design of shallow structures is ongoing. Moreover, and in spite of everything, the use of the dynamic penetrometer with variable energy has not been included in the Eurocodes (soil caractérisation or earthwork control) or in the TC 102 of the ISSMGE. Nevertheless, ISO 22476-2 accepts the use of penetrometers with different, and therefore variable, driving energies, provided that the Dutch formula is used to exploit the measurements taken on site.

5. References

AFNOR. (2012). NF P 94-105 - Sols : Reconnaissance et essais - Contrôle de la qualité du compactage - méthode au pénétromètre dynamique à énergie variable - principe et méthode d'étalonnage du pénétromètre - exploitation des résultats - interprétation.

Angelim, R., Campos, S., Llobet, B., Sales, M., & da Cunha, P. (2016). Correlação Entre Ensaios Spt E Panda 2 (Penetrômetro Leve De Energia Variável) Em Aterro Compactado De Barragem Com Solo. 15 CNG -Congresso Nacional de Geotecnia e 8 CLBG -Congresso Luso-Brasileiro de Geotecnia, 1–12.

ASTM-D6951-18. (2015). Standard Test Method for Use of the Dynamic Cone Penetrometer in Shallow Pavement Applications.

Athapaththu, A. M. R. G., K, Y., & Tsuchida, T. (2016). Geotechnical assessment of natural slopes and valleys based on real time rainfall data. Int. J. of GEOMATE, 10, 1584–1594.

Athapaththu, A. M. R. G., Tsuchida, T., & Kano, S. (2015). A new geotechnical method for natural slope exploration and analysis. Natural Hazards, 75(2), 1327–1348. https://doi.org/10.1007/s11069-014-1384-0

Athapaththu, A. M. R. G., Tsuchida, T., Suga, K., & Kano, S. (2007). A Lightweight Dynamic Cone Penetrometer for Evaluation of Shear Strength of Natural Masado Slopes. Doboku Gakkai Ronbunshuu C, 63(2), 403–416. https://doi.org/10.2208/jscejc.63.403

Benz Navarrete, M. A., Escobar Valencia, E. J., Gourvès, R., Haddani, Y., Breul, P., & Bacconnet, C. (2013). Mesures dynamiques lors du battage pénétromètrique – Détermination de la courbe charge-enfoncement dynamique en pointe. Proceedings of the 18th International Conférence on Soil Mechanics and Geotechnical Engineering, 499–502.

Benz Navarrete, M., Breul, P., & Gourvès, R. (2021). Application of wave equation theory to improve dynamic cone penetration test for shallow soil characterisation. Journal of Rock Mechanics and Geotechnical Engineering. https://doi.org/10.1016/j.jrmge.2021.07.004

Benz-Navarrete, M. A. (2009). Mesures dynamiques lors du battage du penetromètre Panda 2.

Benz-Navarrete, M. A., Breul, P., & Arancibia, G. V. (2020a). Correlation between static (CPT) and dynamic variable energy (Panda) cone penetration tests. 6th International Conference on Geotechnical and Geophysical Site Characterization.

Benz-Navarrete, M. A., Breul, P., & Arancibia, G. V. (2020b). Correlation between static (CPT) and dynamic variable energy (Panda) cone penetration tests. 6th International Conference on Geotechnical and Geophysical Site Characterization.

Broms, B., & Flodin, F. (1988). History of soil penetration testing. Proceedings ISOPT1, Orlando, U.S.A., 1, 157–220.

Butcher, A. P., McElmeel, K., & Powell, J. J. M. (1996). Dynamic probing and its use in clay soils. In Advances in site investigation practice (pp. 383–395). https://doi.org/10.1680/aisip.25134.0032

Chaigneau, L. (2001). Caracterisation des mileux granulaires de surface al'aide d'un penetrometre [Phd dissertation]. Université Blaise Pascal.

Deplagne, F., & Bacconnet, C. (1993). Analyse structurale d'une digue en argile. Compte-Rendu Des Journées de Géostatistique, 181–188.

Escobar Valencia, E. J. (2015). Mise au point et exploitation d'une nouvelle technique pour la reconnaisance des sols : le PANDA 3 [University of Clermont-Auvergne]. https://tel.archives-ouvertes.fr/tel-01519486

Espinace, R., Palma, J., Peña, Á., Villavicencio, G., Boissier, D., Bacconnet, C., & Gourves, R. (2007). The Panda penetrometer: A new alternative for the compaction control of tailing dams.

Goldmann, N. (1699). Comprehensive guidelines to the art of building (Vollständige Anweisung zu der Civil Bau-Kunst).

Gourvès, R. (1991). Le PANDA : pénétromètre dynamique léger à énergie variable pour la reconnaissance des sols.

Gourvès, R., & Zhou, S. S. (1997). The in-situ characterization of the mechanical properties of granular media with the help of penetrometer. In R. P. Behringer & J. T. Jenkins (Eds.), 3rd International conference on micromecanique of granular media (pp. 57–60). Bankelma.

IMANOR. (2019). Contrôle de la qualité du compactage - Méthode au pénétromètre dynamique à énergie variable. Principe et méthode d'étalonnage du pénétromètre. Exploitation des résultats Interprétation.

INN-NCH3261. (2012). Depósitos de relave - Control de compactación con penetrómetro dinámico ligero.

ISO-22476-2. (2005a). Reconnaissance et essais géotechniques — Essais en place — Partie 2: Essais de pénétration dynamique.

Jayawickrama, P. W., Amarasiri, A. L., & Regino, P. E. (2000). Use of dynamic cone penetrometer to control compaction of granular fill. Transportation Research Record, 1736, 71–80. https://doi.org/10.3141/1736-10

Kang, M., Wang, H., Qamhia, I. I. A., Tutumluer, E., Haddani, Y., & Bankston, A. (2023). Degraded Ballast Stiffness Characterization Using Bender Element Field Sensor and PANDA® Penetrometer. Transportation Research Record: Journal of the Transportation Research Board. https://doi.org/10.1177/03611981231156936

Künzel, E. (1936). Der Prüfstab, ein einfaches Mittel zur Bodenprüfung (The Test Rod, a simple tool for soil testing). Bauwelt, 14, 327–329.

Langton, D. D. (1999). The Panda lightweight penetrometer for soil investigation and monitoring material compaction. Ground Engineering, 32, 33–37.

Lepetit, L. (2004). Etude d'une méthode de diagnostic de digues avec prise en compte du risque de liquéfaction [Phd Dissertation, Université Blaise pascal]. https://tel.archives-ouvertes.fr/tel-00006665

Livneh, M., & Livneh, N. A. (2013). The use of the dynamic cone penetrometer for quality control of compaction operations. International Journal of Engineering Research in Africa, 10, 49–64. https://doi.org/10.4028/www.scientific.net/JERA.10.49

López Retamales, S. (2022). Development of a method to evaluate the risk of liquefaction of sands from a dynamic penetrometer test [Phd]. Ecole des Ponts ParisTech.

Lopez Retamales, S., Benz Navarrete, M. A., & Moustan, P. (2019). Comparación de los ensayos de penetración de cono dinámico (DCP) y penetrómetro de cono dinámico de energía variable PANDA®. https://doi.org/10.3233/STAL190206

López Retamales, S., Dupla, J.-C., Canou, J., & Benz Navarrete, M. (2021). Evaluation of soil liquefaction resistance with variable energy dynamic penetration test, PANDA®: state of the art. 6th International Conference on Geotechnical and Geophysical Site Characterization:

Lunne, T., Powell, J. J. M., & Robertson, P. K. (1997). Cone Penetration Testing in Geotechnical Practice (C. Press, Ed.).

Massarch, K. R. (2014). Cone Penetration Testing – A Historic Perspective. In Proc.of 3rd International Symposium on Cone Penetration Testing, 97–134.

Powell, J. (2017). James K. Mitchell Lecture - In-situ testing – Ensuring Quality in equipment, in operation and in interpretation. 19Th International Conference on Soil Mechanics and Geotechnical Engineering.

Retamales, S., Canou, J., Dupla, J.-C., & Navarrete, M. (2021). Development of a liquefaction risk assessment methodology using an instrumented lightweight dynamic penetrometer: calibration chamber tests.

Sabtan, A. A., & Shehata, W. M. (1994). Le pénétromètre mackintosh utilisé comme outil de reconnaissance. Bulletin of the International Association of Engineering Geology - Bulletin de l'Association Internationale de Géologie de l'Ingénieur, 50(1), 89–94. https://doi.org/10.1007/BF02594960

Salgado, R., & Yoon, S. (2003). Dynamic Cone Penetration Test (DCPT) for Subgrade Assessment.

Sanglerat, G. (1972). The penetrometer and soil exploration. Developments in geotechnical engineering. Elsevier.

Sanhueza, C., & Villavicencio, G. (2010). Estimación de parámetros resistentes a partir del ensayo de penetración PANDA y su aplicación en el cálculo de la capacidad de soporte y asentamientos del suelo de fundación (1a parte). Revista de La Construccion, 9(1), 120–131. https://doi.org/10.4067/s0718-915x2010000100013

Sastre Jurado, C. (2018). Exploitation du signal pénétrométrique pour l'aide à l'obtention d'un modèle de terrain [Phd Dissertation]. Université Clermont Auvergne.

Sastre Jurado, C., Benz Navarrete, M. A., Gourvès, R., Breul, P., & Bacconnet, C. (2016). Automatic methodology to predict grain size class from dynamic penetration test using neural networks. Proceedings of the 5th International Conference on Geotechnical and Geophysical Site Characterisation, ISC 2016, 2, 1465–1470.

Sastre Jurado, C., Breul, P., Bacconnet, C., & Benz Navarrete, M. A. (2021). Probabilistic 3D modelling of shallow soil spatial variability using dynamic cone penetrometer results and a geostatistical method. Georisk, 15(2), 139–151. https://doi.org/10.1080/17499518.2020.1728558

Scala, A. J. (1956). Simple methods of flexible pavement design using cone penetrometers. Australia New Zealand Conference On Soil Mechanics and Foundation Engineering, 33–44.

Schmertmann, J. H., & Palacios, A. (1979). Energy Dynamics of SPT. Journal of the Geotechnical Engineering Division, 105(8), 909–926.

Sowers, G., & Hedges, C. (1966). Dynamic Cone for Shallow In-Situ Penetration Testing. In ASTM (Ed.), Vane Shear and Cone Penetration Resistance Testing of In-Situ Soils, (p. 29). https://doi.org/10.1520/STP44629S

Tsuchida, T., Athapaththu, A., K., Kano, S., & Suga, K. (2011). Estimation of In-Situ Shear Strength Parameters of Weathered Granitic (Masado) Slopes Using Lightweight Dynamic Cone Penetrometer. Soils and Foundations -Tokyo-, 51(3), 497–512.

Villavicencio, G. (2009). Methodologie pour evaluer la stabilite des barrages de residus miniers. Université Blaise Pascal.

Villavicencio, G., Bacconnet, C., Valenzuela, P., Palma, J., Carpanetti, A., Suazo, G., Silva, M., & García, J. (2022). The Use of Lightweight Penetrometer PANDA for the Compaction Control of Classified Sand Tailings Dams. Minerals, 12(11). https://doi.org/10.3390/min12111467

Villavicencio, G., Breul, P., Bacconnet, C., Boissier, *-Daniel, & Espinace, R. (2011). Estimation of the variability of tailings dams properties in order to perform probabilistic assessment. Geotechnical and Geological Engineering, 29(6), 1073.

Villavicencio, G., Breul, P., Bacconnet, C., Fourie, A., & Espinace, R. (2016). Liquefaction potential of sand tailings dams evaluated using a probabilistic interpretation of estimated in-situ relative density. Revista de La Construccion, 15(2), 9–18. https://doi.org/10.4067/s0718-915x2016000200001

Villavicencio, G., Suazo, G., Rojas, S., Zuñiga, R., Universidad, P., & Valparaíso, C. De. (2018). The Effects of Confining Pressure, Density and Tailings Water Content on the Cone Resistance of Dynamic Lightweight Penetrometers. Tailings 2018, 1–9.

Villavicencio, G., Suazo, G., Zuñiga, R., & Valenzuela, P. (2021). Effects of Soil Conditions on the Cone Resistance of Lightweight Penetrometers. Journal of Geotechnical and Geoenvironmental Engineering, 147(7). https://doi.org/10.1061/(asce)gt.1943-5606.0002531

Waschkowski, E. (1983). Essais de pénétration – Le pénétromètre dynamique. Bulletin Liaison Laboratoire de Ponts et Chaussées, 125, 95–103.

Webster, S. L., Grau, R. H., & Williams, T. P. (1992). Description and Application of Dual Mass Dynamic Cone Penetrometer.

Zhou, S. S. (1997). Caracterisation des sols de surface à l'aide du penetrometre dynamique leger a energie variable type P.A.N.D.A. University Blaise Pascal, Clermont Ferrand, France.